Electrodeposition of Co-Ni-Mo_xO_y Powders: Part I. The Influence of Deposition Conditions on Powder Composition and Morphology

JASMINA STEVANOVIĆ, JASNA STAJIĆ-TROŠIĆ, VLADAN ĆOSOVIĆ, VLADIMIR PANIĆ, OLIVERA PEŠIĆ, and BRANKA JORDOVIĆ

The Co-Ni-Mo_xO_y powders were obtained electrochemically at a constant current density from ammonia electrolyte. Ni and Co were anomalously deposited, inducing Mo deposition, which cannot be deposited separately from aqueous solutions. The obtained Co-Ni-Mo_xO_y powders were investigated by energy dispersive spectroscopy (EDS), X-ray diffraction (XRD), and scanning electon microscope (SEM) methods. Based on the obtained experimental results, it was concluded that the particle size of deposited powders is influenced by the chemical composition of the electrolyte and current density imposed. XRD results suggested that obtained powders were of amorphous structure, although a Co_3Mo compound can be formed if certain experimental conditions are applied.

DOI: 10.1007/s11663-009-9305-4

I. INTRODUCTION

ELECTROCHEMICALLY deposited alloys of iron-group metals (Fe, Co, and Ni), in a form of powders or coatings, are important magnetic materials[1–14] as well as good catalysts for hydrogen evolution.[15–17] Powders of binary and multicomponent alloys as well as single metal deposits are classified in a system defined by Brenner[18] based on the type of deposition the metals may undergo. If more electronegative metal is favored during the deposition of an alloy, then the deposition process is called anomalous deposition. Iron-group metals are deposited anomalously in the presence of Zn or among each other from the solutions of their simple and complex salts. Electrochemical deposition of more noble metal can be inhibited because the less noble metal starts to deposit preferentially at a certain potential.

However, certain elements, like Mo, W, and Ti, cannot be obtained electrochemically from the aqueous solutions.[19] Electrochemical deposition of these metals is induced by codeposited iron-group metals. This induced codeposition has some characteristics that make it distinguishable from the other deposition techniques, such as a limited amount of the element being deposited inductively.

JASMINA STEVANOVIĆ, JASNA STAJIĆ-TROŠIĆ, and VLADIMIR PANIĆ, PhDs, are with the Department of Electrochemistry, Institute of Chemistry, Technology and Metallurgy, 11000 Belgrade, Serbia. VLADAN ĆOSOVIĆ, PhD, is with the Department of Materials and Metallurgy, Institute of Chemistry, Technology and Metallurgy, 11000 Belgrade, Serbia. Contact e-mail: vlada@tmf.bg.ac.rs OLIVERA PEŠIĆ, MSc, and BRANKA JORDOVIĆ, PhD, are with the Technical Faculty Čačak, University of Kragujevac, Svetog Save 65, 32000 Čačak, Serbia.

Manuscript submitted March 25, 2009.
Article published online September 29, 2009.

Numerous different hypotheses focus on the mechanism of the induced deposition. The hypothesis for molybdenum and tungsten depolarization as a result of alloying (*i.e.*, the formation of a solid solution or an intermetallic compound was introduced[20]), which is based on the fact that molybdenum and tungsten alloys deposit at more positive potential than the metals that induce their deposition.

One of the other mechanisms is based on the hypothesized formation of a mixed complex ion that contains tungsten and iron-group metal in the electrolyte for deposition.[21] Depolarization may take place, because the reduction of these metals from their mixed complex ions is favored thermodynamically with respect to the reduction of each metal ion. Polarographic investigations suggest the presence of the Ni complex with tungstenites, from which tungsten is reduced completely to the pure metal or reduced partially to an oxide of tungsten with lower valence.

During the reduction of pure molybdates and tungstenites from the aqueous solutions, the products of mixed oxidation states between the hexavalent and pure metal are deposited on the cathode. Therefore, the hypothesis about the presence of oxide film on the cathode is based on the assumption that the oxide layer of partially reduced molybdenum and tungsten oxides is being reduced in reaction with hydrogen that is adsorbed on freshly deposited iron-group metals.[22,23] This catalytic reduction mechanism also assumes that the number of hydrogen atoms adsorbed on iron-group metals is equal to the number of unpaired electrons.

Golbukov and Jurev[24] reported that, in the deposition process of Mo with Fe and Ni, the reduction of molybdates from the solution, and the formation of the layer of insoluble compounds of lower valence, most probably Mo (III) oxide/hydroxide, take place. A formed oxide layer has lower permeability for Fe (II)

and Ni (II) ions, which causes the reduction of these ions to take place at higher overvoltages. The reduction process is influenced by the ratio of two consecutive reactions that are as follows: (1) the reduction of molybdenum (VI) ions with the formation of a layer of molybdenum compounds with a lower valence and (2) the reduction of the formed oxide layer by nickel and iron following the deposition of alloy powders.

Investigations of the mechanism of induced codeposition of Ni and Mo by electrochemical impedance spectroscopy (EIS) have shown that the multistage reduction of molybdates occurs with the participation of iron-group metals.[25]

The studies of the mechanism of Mo deposition with the Ni from the citrate electrolytes have led to the hypothesis of adsorption and reduction of molybdate ion species.[26–29] According to this model, the reduction of bivalent Ni from the complex is controlled by the transport processes and the two-stage reduction that includes the presence of the adsorbed intermediate. In parallel, molybdate is catalytically reduced through an adsorbed Ni–Mo intermediate. In relation to this mechanism, Ni^{2+} (aq) ion species act as catalysts for molybdate reduction, which forms the adsorbed reaction intermediate $[Ni^{2+}(aq)MoO_2]_{ads}$. Mo is deposited *via* a reduction of the reaction intermediate, and at the same time, the two Ni^{2+} are being regenerated. The reduction of Ni and Mo takes place through two parallel reactions.

Bearing in mind these considerations, different preparation conditions lead to considerable difference in structure, morphology, and composition of deposited powders, which can affect their magnetic and electrocatalytic properties. The aim of this study is to investigate how electrolyte composition and electrochemical parameters in the deposition process affect the composition and structure of prepared powders as well as to investigate how these features affect magnetic properties of this material, which will be presented in part II of this article.

II. EXPERIMENTAL

The powders were electrodeposited from the electrolyte that contained the following: $CoSO_4$, $NiSO_4$, $(NH_4)_6Mo_7O_{24}$, NH_4Cl, and NH_4OH. Two Ni^{2+}/Co^{2+} concentration ratios were used: 1:1 [0.1M Ni/0.1 M Co] and 4:1 [0.16 M Ni/0.04 M Co]. The molybdate concentration also was varied from 0.005 to 0.06 mol/dm^3, whereas the NH_4Cl concentration was 74.13 g/dm^3. The NH_4OH was added to keep the pH value at 10.6.

The influence of Co, Ni, and Mo concentrations in electrolyte on the electrochemical parameters of deposition was investigated as well as the influence of the current density (200–800 mA/cm^2) on the morphology and composition of deposited Co-Ni-Mo_xO_y powders.

Polarization curves were recorded in a standard electrochemical cell with a Ti working electrode (0.5-cm-thick plate with the surface area of 32 cm^2), a platinum foil or Pb/PbO_2 counter electrode, and a saturated Ag/AgCl electrode for reference. Polarization measurements were performed using a EG & G PAR 273 A potentiostat (Princeton, NJ) with the sweep rate of 1 mV/s.

The electrochemical cell with a total volume of 5.5 dm^3 used for deposition had a separate Luggin capillary compartment. During the deposition, the temperature was kept constant at 25 °C. The solutions for deposition were prepared from analytical grade chemicals and twice-distilled water. After deposition, obtained Co-Ni-Mo_xO_y powders were rinsed with distilled water, and 0.1 pct benzoic acid solution then left to dry at 110 °C.

The morphology and the particle size of the electrodeposited powders were observed using a scanning electron microscope (SEM) JEOL JSM-6460 LV (Tokyo, Japan).

The energy dispersive spectroscopy (EDS) analysis was carried out on the Oxford Instruments-INCA Energy system (Oxfordshire, UK), which provided the composition of the deposited Co-Ni-Mo-O alloy powders.

The phase composition of the obtained powders was determined by the X-ray diffraction (XRD) analysis performed on an X'Pert PRO MPD multipurpose X-ray diffraction system from PAN analytical (ALEMO, the Netherlands). Data were collected in a 2θ 0.02 deg step scan mode between 20 and 110 deg.

III. RESULTS AND DISCUSSION

During the codeposition of Co and Ni from ammoniacal electrolyte, anomalous Ni deposition occurred. The equilibrium potential of Ni is 20 mV greater than the equilibrium potential of Co. The polarization curves of the electrochemical deposition of single metals show that pure Ni deposition takes place at the potential for about 100 mV less than Co deposition (Figure 1, curves 1 and 2).

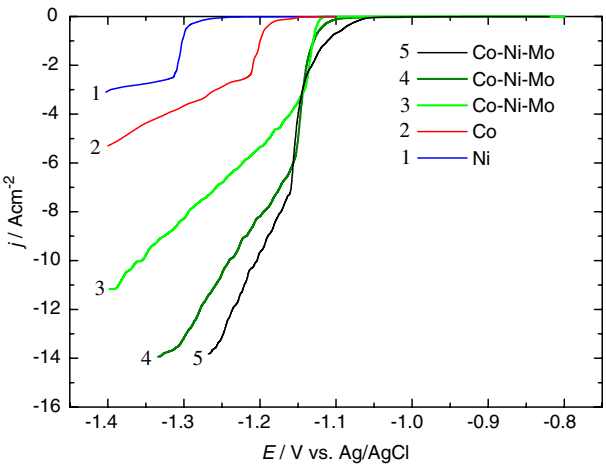

Fig. 1—Polarization curves for the electrodeposition of the following: 1) pure Ni; 2) pure Co; 3) Co-Ni-Mo_xO_y powder from 0.03 M Mo solution; 4) Co-Ni-Mo_xO_y powders deposited the solution containing 0.01 M Mo; 5) Co-Ni-Mo_xO_y powders deposited the solution containing 0.005 M Mo.

In the buffered ammoniacal electrolyte, with a pH of 10.6, the influence of all ligands but ammonia is negligible, so that Co and Ni only are present as complex ions of octahedral type that are as follows: $[Co(NH_3)_6]^{2+}$ and $[Ni(NH_3)_6]^{2+}$ with a stability constant of $10^{4.39}$ and $10^{8.01}$, respectively. These values of stability constants indicate that Co will be deposited more easily than Ni, because of the lower stability of the Co complex ion. The anomalous deposition of Ni is the consequence of a significantly higher affinity of the Ni ion to create complexes so that its deposition potential becomes considerably more negative in comparison with the essentially less noble Co.

The polarization curve of the Co-Ni alloy powder deposition lies between the polarization curves of the deposition of pure Co and Ni powders, and its position depends on the Ni^{2+}/Co^{2+} concentration ratio in the electrolyte. Practically, for the Ni content to be higher than the Co content in the deposit, the Ni^{2+} concentration in the electrolyte has to be significantly higher than the Co^{2+} concentration.[14] Although, Ni and Co powders as well as the Ni-Co alloy powders by themselves are not the subject of this research, the conditions of the deposition of these powders were studied to clarify the mechanism of Co-Ni-Mo_xO_y powder deposition and to determine which of the iron-group metals, Co or Ni, preferentially influences the Mo deposition from the ammoniacal electrolyte.

Molybdenum was introduced into the electrolyte for deposition as $[MoO_4]^{2-}$. Despite its affinity to form poly-ions or clusters like $[Mo_7O_{24}]^6$, which is detected in a solution with a pH higher than 9 by diffuse reflection spectroscopy, Mo was present in the solution preferentially used for deposition (pH 10.6) in a form of molybdates. If the pH of the solution was adjusted to values lower than 5, then Mo poly-ions were formed.[30] The investigation of the Mo-containing powder deposition from the ammoniacal electrolyte strongly supports the mechanism *via* adsorption and catalytic reduction of molybdate species hypothesis.[26–29] However, some corrections in the terminology should be made. Iron-group metals induce the Mo deposition, whereas Mo acts simultaneously as a catalyst for the deposition of iron-group metals. Mo causes the deposition potentials of pure Ni and Co to be more positive with about 200 and 100 mV, respectively, compared with Mo-absent electrolytes (Figure 1, curves 1 and 2). Electrodeposition of pure Ni and Co from the ammoniacal electrolyte starts at the potentials less than −1.3 and −1.2 V, respectively, whereas Co-Ni-MoxOy powder starts to deposit at a slightly more positive potential than those potentials of pure metals—*i.e.*, at about −1.1 V.

However, recorded polarization curves 3, 4, and 5 for Co-Ni-Mo_xO_y powder (Figure 1) show that the increase of the Mo concentration in the electrolyte shifts the deposition potential of Co-Ni-Mo_xO_y powder to more negative values and lowers the plateau of limiting deposition current density. From the electrolyte that contains 0.0005 M Mo, alloy powder deposition starts at the potential of −1.07 V (Figure 1, curve 5), whereas deposition of the alloy from the electrolyte containing 0.03 M Mo starts at the potential that is 100 mV less (−1.123 V) (Figure 1, curve 3). The limiting deposition current density is 7.183 A/cm^2 for 0.005 M Mo and 2.911 A/cm^2 for 0.03 M Mo.

The deposition mechanism suggested elsewhere[26–29] is considered to be the most probable in this study only for the basic electrolytes when Mo is present in a form of molybdates but not in acidic electrolytes where Mo is present in a form of poly-ions. According to this mechanism, Ni and Co should deposit in a two-step reduction, whereas Mo should deposit in a form of pure metal, oxide, or even compound with Ni and/or Co. Adsorbed reaction intermediates should be $[Co^{2+}(aq)\text{-}MoO_2]_{ads}$ and/or $[Ni^{2+}(aq)MoO_2]_{ads}$. Because of greater stability of the Ni ammoniacal complex with respect to molybdate one, lower Ni content in the deposit also should be expected, becuase it is confirmed by experimental results. However, the results of the EDS analysis presented in Tables I, II and III indicate that the Ni content in the deposit nearly is independent of the current density and Ni concentration. By increasing the Ni^{2+}/Co^{2+} concentration ratio to 4:1, the Ni content in the deposit is increased only by 1-2 pct (Table III). Therefore, Co preferentially induces Mo deposition and that the influence of Ni is almost negligible.

In the Co-Ni-Mo_xO_y powder, Mo can be present in a form of pure metal, oxide (MoO, Mo_2O_3, MoO_2, MoO_3, and Mo_2O_5) or even as a compound with Co and/or Ni.

Table I. The Chemical Composition of Electrodeposited Co-Ni-Mo-O Alloy Powders (Ni^{2+}/Co^{2+} (1:1), 400 mA/cm^2)

Mo Concentration in the Electrolyte (mol/L)	O (at. pct)	Co (at. pct)	Mo (at. pct)	Ni (at. pct)
0.005	72	11	14	3
0.01	62	15	30	3
0.03	44	18	36	2
0.06	44	18	36	2

Table II. The Chemical Composition of Electrodeposited Co-Ni-Mo-O Alloy Powders (Ni^{2+}/Co^{2+} (1:1), 800 mA/cm^2)

Mo Concentration in the Electrolyte (mol/L)	O (at. pct)	Co (at. pct)	Mo (at. pct)	Ni (at. pct)
0.005	63	12	22	3
0.01	50	16	32	2
0.03	42	19	37	2

Table III. The Chemical Composition of Electrodeposited Co-Ni-Mo-O Alloy Powders (Ni^{2+}/Co^{2+} (4:1), 400 mA/cm^2)

Mo Concentration in the Electrolyte (mol/L)	O (at. pct)	Co (at. pct)	Mo (at. pct)	Ni (at. pct)
0.005	68	12	14	6
0.01	68	12	15	5
0.03	67	13	17	3

The adsorbed intermediate is most likely $[Co(NH_3)_6Mo_xO_y]^{2+}_{ads}$ and/or $[Ni(NH_3)_6Mo_xO_y]^{2+}_{ads}$, where $x \geq 1$ and $y \geq 0$, but $[Co(NH_3)_6Mo_xO_y]^{2+}_{ads}$ is more abundant. This complex cation prevents the Ni transport from the electrolyte to the surface of the electrode, and at the same time, it facilitates unaffected Co and Mo deposition. Owing to a higher stability constant ammoniacal complex of Ni than Co, Ni most likely cannot form complex cation with Mo in the presence of Co, which would make Co deposition in the form of a compound with Mo, oxide, or pure metal much easier.

The approximate chemical compositions of the deposited powders determined by the EDS analysis carried out on several different regions of each individual sample are presented in Tables I, II and III.

The presented results of EDS analysis of the deposited alloy powders suggest that every increase of the Mo content in the deposit is accompanied by an increase in the Co content, whereas the Ni content is independent of Ni^{2+}/Co^{2+} concentration.

Large agglomerates were formed and are depicted in Figures 2 and 3.

Larger grains were deposited at the 1:1 Ni^{2+}/Co^{2+} concentration ratio (0.1 M Ni, 0.1 M Co) with a current density of 400 mA/cm^2 (Figure 2(a)) than with a current density of 800 mA/cm^2 (Figure 2(c)).

The powder deposited from the electrolyte 0.03 M Mo (Figure 2(b)) with a current density of 800 mA/cm^2, comprised larger grains, whereas the conditions with a current density of 400 mA/cm^2 and a higher Mo concentration (0.06 M) favor the deposition of smaller grains (Figure 2(a)). This pattern shows that an increase in Mo concentration and current density cause the grain to decrease in size.

Figure 3 depicts the alloy powders deposited from the electrolytes with a higher Ni^{2+}/Co^{2+} concentration ratio (4:1) and Mo concentration that ranges from 0.005 to 0.03 M, with a constant current density of 400 mA/cm^2. The decrease in grain size is observed with the increase in Mo concentration in the electrolyte.

Comparing Figures 2 and 3, shows the changes in the morphology of the deposited powders that follow the increase in the Ni^{2+}/Co^{2+} concentration ratio in the electrolyte. The powder deposited from the electrolyte with the 1:1 Ni^{2+}/Co^{2+} concentration ratio (Figure 2) comprises primarily flake-shaped grains, whereas the powders deposited from electrolyte with the 4:1 Ni^{2+}/Co^{2+} concentration ratio (Figure 3) are in the form of large agglomerated particles with a more or less dense cauliflower structure.

The results of the EDS analysis indicate that an increase in the Mo concentration in the electrolyte from 0.005 to 0.03 mol/L at a constant current density (Tables I, II, and III) causes Mo content in the deposit to increase. However, with continued increase in Mo concentration from 0.03 to 0.06 mol/L, the Mo content in the Co-Ni-Mo-O alloy deposit does not change (Table I).

Changes in Ni and Co concentration in the electrolyte for deposition have a significant influence on the

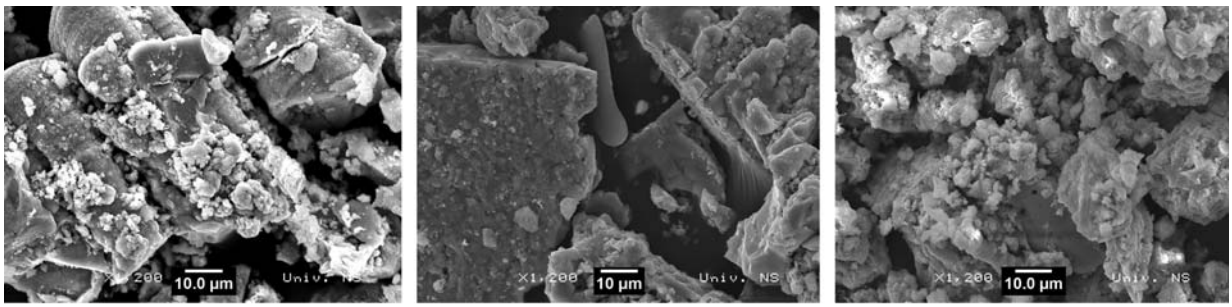

(a) 400 mA/cm^2, (0.06 M) Mo **(b)** 800 mA/cm^2, (0.03 M) Mo **(c)** 800 mA/cm^2, (0.06 M) Mo

Fig. 2—SEM micrographs of Co-Ni-Mo_xO_y powders electrodeposited from the solution that contained 1:1 Ni^{2+}/Co^{2+} (0.1 M Ni, 0.1 M Co).

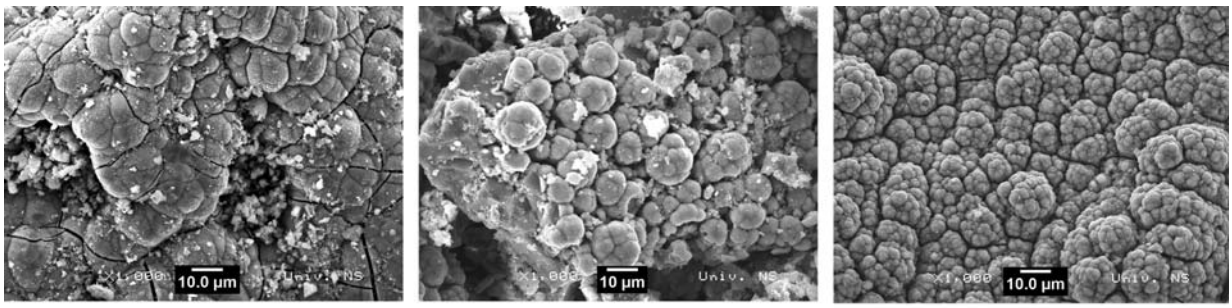

(a) (0.005 M) Mo **(b)** (0.01 M) Mo **(c)** (0.03 M) Mo

Fig. 3—SEM micrographs of Co-Ni-Mo_xO_y powders electrodeposited at the current density of 400 mA/cm^2 from the solution that contained 4:1 Ni^{2+}/Co^{2+} (0.16 M Ni, 0.04 M Co).

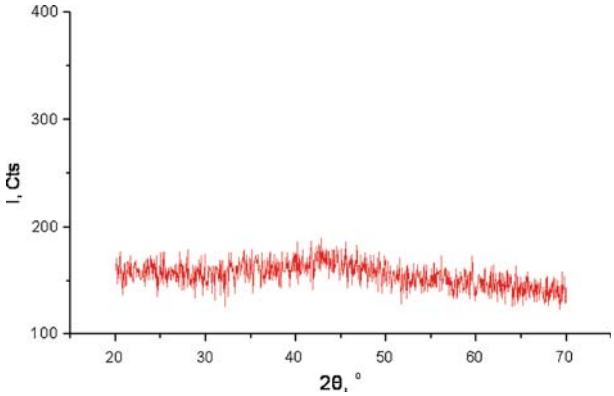

Fig. 4—XRD patterns of Co-Ni-Mo_xO_y powders deposited from the solution that contained 0.1 M Ni, 0.1 M Co (1:1) and 0.06 mol/L Mo, at the current density of 800 mA/cm^2.

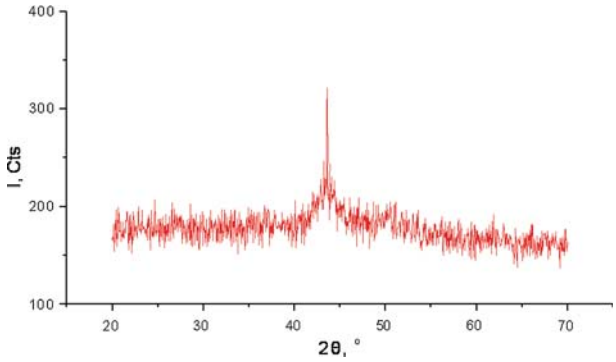

Fig. 5—XRD patterns of Co-Ni-Mo_xO_y powders, deposited from the solution that contained 0.1 M Ni, 0.1 M Co (1:1) and 0.03 mol/L Mo, at the current density of 400 mA/cm^2.

chemical composition of deposited powders, as evident in the results of the EDS analysis presented in Tables I. and III. For the 1:1 Ni^{2+}/Co^{2+} concentration ratio, the increase of Mo concentration in the electrolyte caused a decrease in oxygen and Ni content and an increase in Mo and Co content (Table I).

The increase in the Ni^{2+}/Co^{2+} concentration ratio of 4:1 (0.16 M Ni and 0.04 M Co) caused oxygen and Ni to decrease slightly in the Mo concentration results and caused a negligible increase in Mo content (Table III).

Comparing the results shown in Tables I and III reveals that the content of individual elements (Co, Ni, and Mo) in the deposit obtained from the electrolyte with a higher Ni concentration are significantly lower than with a lower Ni concentration, which suggests that this decrease is related to the increased oxygen content. The results also show that the increase in Co content in all the powder samples is accompanied by an increase in Mo content.

With an increase in the current density from 400 to 800 mA/cm^2 and while keeping other parameters of the system constant, the Mo and Co content in the deposit increase with an increase in Mo concentration in the electrolyte (Tables I and II).

The phase composition of the deposited Co-Ni-Mo_xO_y powders was studied by the X-ray analysis. Figures 4 and 5 depict the X-ray diffractograms of the Co-Ni-Mo_xO_y powders obtained under different deposition conditions. The images indicate that all prepared powders are of amorphous structure.

Generally when lower current densities are applied, the obtained deposits will have larger grains. Also, the larger grains in the deposit occur when the Mo concentration in the electrolyte is lower. The same pattern is observed on the X-ray diffractograms, because the powders deposited from electrolytes with a lower Mo concentration and at lower current densities exhibit higher crystallinity. It is difficult to assign a specific crystalline phase based on the appearance of a single diffraction peak around 2θ 44°. According to the literature data, this peak could correspond with an fcc (Co-Ni) solid solution,[31] with a (002) plane of ε-Co, but also with a (002) plane of Co_3Mo compound.[32]

IV. CONCLUSION

In the ammoniacal electrolyte of pH 10.6, Mo is present only in a form of molybdate ions $[MoO_4]^{2-}$, whereas Co and Ni are present as complex ions of an octahedral type that are as follows: $[Co(NH_3)_6]^{2+}$ and $[Ni(NH_3)_6]^{2+}$ with the stability constant values of $10^{4.39}$ and $10^{8.01}$, respectively. These values indicate that Co will be deposited more easily, because its complex is less stable. Anomalous deposition of Ni is the consequence of the significantly higher affinity of Ni ions to create complexes, so that its deposition potential becomes 120 mV less compared with the less noble metal Co during the deposition of the alloy.

In the Co-Ni-Mo_xO_y powder, Mo can be present as pure Mo in the form of the following oxides: MoO, Mo_2O_3, MoO_2, MoO_3 or Mo_2O_5, as well as in the form of compounds with Co and/or Ni. The adsorbed intermediate is $[Co(NH_3)_6Mo_xO_y]^{2+}_{ads}$ and/or $[Ni(NH_3)_6Mo_xO_y]^{2+}_{ads}$, where $x \geq 1$ and $y \geq 0$. However, $[Co(NH_3)_6Mo_xO_y]^{2+}_{ads}$ is preferentially formed. This complex cation hinders the Ni transport from the solution to the surface of the electrode and at the same time enables unaffected Co and Mo deposition. Because of the stability constant of Ni ammonia complex is about four orders of magnitude higher than the stability constant of the Co ammonia complex, Ni cannot form complex cation with Mo in the presence of Co, which would make its deposition in the form of pure metal, oxide, or compound that contains Mo much easier.

An increase in Co and Mo concentrations in the electrolyte as well as an increase in the current density affects the grain size in the deposit—*i.e.*, smaller particles are obtained.

The increase in Ni concentration in the electrolyte was found to affect the morphology of the Co-Ni-Mo_xO_y powders from primarily flake-shaped angular grains to agglomerated particles with a cauliflower structure. The increase in Ni concentration also lowers the Co and Mo content in the deposit. Additionally, an increase of the Co and Mo content was observed.

With a low current density and lower Mo concentrations in the electrolyte, slightly larger grains of the deposit formed that were identified as a Co_3Mo compound.

Electrochemical deposition of Co-Ni-Mo_xO_y powders is accompanied by the simultaneous hydrogen evolution, which is the primary reaction. Obtained experimental results indicate that current efficiency for powder deposition increases with a decrease in current density.

Future research will be done to determine the qualitative and quantitative phase composition of the obtained Co-Ni-Mo_xO_y powders as well as their magnetic properties. The results of these analyses will be reported in the following paper "Characterization of Co-Ni-Mo-O alloy powders part II."

ACKNOWLEDGMENT

This work was supported by the Ministry of Science of the Republic of Serbia under research projects H142044 and OI142035B.

OPEN ACCESS

REFERENCES

1. P.J. Grundy: *J. Phys. D*, 1988, vol. 31, pp. 2957–90.
2. D.E. Laughlin, B. Lu, Y.N. Hsu, J. Zou, and D.N. Lambeth: *IEEE Trans. Magn.*, 2000, vol. 36, pp. 48–53.
3. M. Takai, K. Hayashi, M. Aoyagi, and T. Osaka: *J. Electrochem. Soc.*, 1997, vol. 144, pp. L203–04.
4. T. Osaka, M. Takai, K. Hayashi, K. Ohashi, and M. Saito: *Nature*, 1998, vol. 392, pp. 796–98.
5. M. Futamoto, N. Inaba, A. Nakamura, and Y. Honda: *Acta Mater.*, 1998, vol. 46, pp. 3777–86.
6. N. Inaba, Y. Uesaka, and M. Futamoto: *IEEE Trans. Magn.*, 2000, vol. 36, pp. 54–60.
7. C. Lin, Y.G. Chen, and B.X. Liu: *Thin Solid Films*, 1999, vol. 338, pp. 314–19.
8. A. Slawska-Waniewska, P. Didukh, H.K. Lachowicz, and T. Kulik: *J. Magn. Magn. Mater.*, 2000, vol. 215, pp. 495–98.
9. A. Inoue, A. Makino, and T. Mizushima: *J. Magn. Magn. Mater.*, 2000, vol. 215, pp. 246–52.
10. O. Gutfleisch: *J. Phys. D*, 2000, vol. 33, pp. R157–72.
11. I.C. Tung, H.W. Zhang, S.Y. Yao, J.C. Shih, B.G. Shen, and T.S. Chin: *J. Phys. D*, 1999, vol. 32, pp. 1587–90.
12. B. Bordin, G. Buttino, A. Cecchetti, and M. Poppi: *J. Phys. D*, 1999, vol. 32, pp. 1795–800.
13. I. Nicolov, R. Darkaoui, E. Zhecheva, R. Stoyanova, N. Dimitrov, and T. Vitanov: *J. Electroanal. Chem.*, 1997, vol. 429, p. 157.
14. V.D. Jovic, B.M. Jovic, and M.G. Pavlovic: *Electrochim. Acta*, 2006, vol. 51, pp. 5468–77.
15. M.M. Jaksic: *Electrochim. Acta*, 1984, vol. 29, p. 1539.
16. M.M. Jaksic: *Int. J. Hydrogen Energy*, 1986, vol. 11, pp. 519–32.
17. J. Liu, W.H. Wang, and S.H. Ye: *J. Alloys Compd.*, 1999, vol. 285, pp. 263–66.
18. A. Brenner: *Electrodeposition of Alloys; Principles and Practice*, Academic Press, New York, NY, 1963.
19. D. Landolt: *Electrochim. Acta*, 1994, vol. 39, p. 1075.
20. T.F. Frantsevich-Zabludovskaya and A.I. Zayats: *Zhurn. Priklad. Khim.*, 1957, vol. 30, p. 723.
21. W.E. Clark and M.H. Leitzke: *J. Electrochem. Soc.*, 1952, vol. 99, p. 246.
22. D.W. Ernst and M.L. Holt: *J. Electrochem. Soc.*, 1958, vol. 105, p. 686.
23. H. Fukushima, T. Akiyama, S. Agaki, and K. Higashi: *Trans. Jpn Inst. Metals*, 1979, vol. 20, p. 358.
24. L.A. Golubkov: *Yurev, Zhurn. Priklad. Khim.*, 1971, vol. 44, p. 2419.
25. E. Chassaing, K. Vu Quang, and R. Wiart: *J. Appl. Electrochem.*, 1989, vol. 19, p. 839.
26. E.J. Podlaha and D. Landolt: *J. Electrochem. Soc.*, 1996, vol. 143, p. 885.
27. E.J. Podlaha and D. Landolt: *J. Electrochem. Soc.*, 1996, vol. 143, p. 893.
28. E.J. Podlaha and D. Landolt: *J. Electrochem. Soc.*, 1997, vol. 144, p. 1672.
29. D. Landolt, E.J. Podlaha, and N. Zech: *Zeitsch. Physik. Chem.*, 1999, vol. 208, p. 167.
30. O.N. Kononova, S.V. Kachin, A.E. Chaikovskaya, A.G. Kholmogorov, and O.P. Kalyakina: *Turk. J. Chem.*, 2004, vol. 28, p. 193.
31. E.M. Arce-Estrada, V.M. Lopez-Hirata, L. Martinez-Lopez, H.J. Dorantes-Rosales, M.L. Saucedo-Munoz, and F. Hernandez-Santiago: *J. Mat. Sci.*, 2003, vol. 38, p. 275.
32. C.-F. Chu and S.-T. Wu: *Mat. Chem. Phys.*, 2001, vol. 71, p. 248.